TBM Tuyeres Arrangements and Flow – Comparison Between BOF Ternium Brasil and Cold Model







Authors

Breno T. Maia (first row, left)
technical and commercial director BOF, Lumar Metals, Santana do Paraíso, MG, Brazil
breno.totti@lumarmetals.com.br

Caio N.A. Diniz (first row, right)
continuous casting process engineer, Ternium Brasil, Rio de Janeiro, RJ, Brazil
caio.diniz@ternium.com.br

Daniel Carvalho (second row, left)
BOF metallurgical process engineering, Ternium Brasil, Rio de Janeiro, RJ, Brazil
daniel.carvalho@ternium.com.br

Daniela L. de Souza (second row, right)
metallurgical engineer intern, Universidade Federal de Minas Gerais

José Artur A. de Guimarães (third row, left)
metallurgical engineer intern, Universidade Federal de Minas Gerais

Raissa S. Salgado (third row, right)
metallurgical engineer intern, Universidade Federal de Minas Gerais

Roberto P. Tavares (fourth row)
professor, Universidade Federal de Minas Gerais, Belo Horizonte, MG, Brazil
rtavares@demet.ufmg.br

Primary steelmaking through BOF converters represents an important point in steel production. Against a challenging and competitive market, operational stability and innovations are necessary to reach quality and suitable costs. In order to study the combined blowing through a cold physical model, in similarity with Ternium Brasil's 330-ton converter, visual inspection and colorimetry methods were used to define the jet penetration and the best tuyere configuration, respectively, on the metal bath behavior. A bath lance distance was found that decreases mix time with low slopping probability. After cold model results, parameters can be recalculated for industrial practice with good agreement.

Facing a challenging and competitive steel scenario, mills are constantly seeking improvements in the process, aiming for high-quality steel production, associated with the reduction of process costs. In order to better develop production, new technologies and techniques are implemented in the industrial plant, such as the emergence of the combined blow in the BOF converter. The inert gas injection introduction from the bottom of the converter (Thyssen blowing metallurgy, or TBM) increases the metal bath agitation, reducing zones of chemical stagnation, while favoring the dephosphorization and reducing the iron in the slag. In this way, it is interesting to improve the study of the blow parameters, lance flow, nozzle number and torsion angle, DBL (distance of the bath lance), flowrate and tuyere arrangement. Through physical modeling techniques, it is possible to recreate small-scale reactor models that can be operated in the laboratory, at a much lower cost than an experiment in an industrial plant, avoiding problems such as a fall in operational routine. Considering the similarity realized through the dimensionless numbers, it is possible to transpose the results obtained in the cold model (operated in laboratory) to the industrial reactor of Ternium BR, shown in Fig. 1. In this project,

Figure 1

Ternium Brasil converter (330 ton).

Figure 2

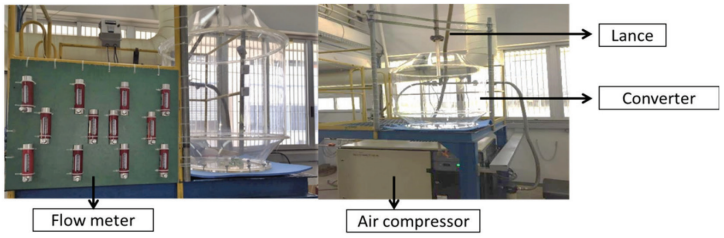

LaSiP structure (Process Simulation Laboratory).

the main objectives are the jet penetration analysis, the decarburization area measurement, verification of the jet and tuyere influence, and kinetic study of the process, during combined blow.

Experimental Procedure

In the LaSiP-UFMG laboratory, the experiments were carried out in a cold model of BOF converter similar to that of Ternium BR with 12 air injection points in the bottom, constructed at a $^1/_{10}$ scale (Fig. 2).

It is noteworthy that the laboratory flow values were determined from a conversion using the modified Froude number, expressed in Eq. 1:

$$Fr^* = \frac{\rho_{gas} \times V_{EXIT}{}^2 \times D_{EXIT}{}^2 \times \cos\theta \times n}{\rho_{STEEL} \times g \times DBL^3} \quad \text{(Eq. 1)}$$

where

Fr^* = modified Froude number LaSiP, relation between forces of inertia and gravitational forces,
g = acceleration of gravity ($m.s^{-2}$),
ρ_{steel} = density of the bath ($kg.m^{-3}$),
ρ_{gas} = gas density at nozzle outlet ($kg.m^{-3}$),
V_{EXIT} = speed at nozzle outlet (m/second),
D_{EXIT} = nozzle outlet diameter (m/second),
θ = output angle with vertical and
n = number of nozzles.

It can be observed that, contrary to what happens in industrial practice, in laboratory experiments the lance rises in the final blow stage (DBL increases). This fact can be explained due to a compensation relation between the flow and the DBL.

The tests simulated two blowing steps performed at Ternium BR, being the decarburization and the blowing end, as shown in Table 1.

Mixing Time — Colorimetric Analysis — Using front and lower footage, the mixing times were analyzed by the colorimetric method. This method consists of the addition of a tracer, potassium permanganate, which presents a strong coloration distinct from that presented by the bath (water), so that its mixing behavior can be observed in the bath from the moment of its addition. The gap time in which the plotter takes to reach practically the entire bath is considered the mixing time.

Jet Penetration and Decarburization Area — From the frontal filming performed for each experiment, images were obtained from three different moments of the blow, making it possible to measure, from the ImageJ® software (Fig. 3), the jet penetration length and the decarburization area generated in the jet impact with the bath. The height of the static water bath (200 mm) was used as the input scale of the program, being a reference for the various possible delimitations offered by the software.

CO_2 Desorption — The CO_2 desorption of a caustic soda solution was used to simulate the decarburization rate at the end of the blow. The pH of the bath was measured after the addition of a NaOH solution of known concentration to give the initial pH. A small amount of phenolphthalein was also added. CO_2 was then injected into the bath until the pH reached approximately 6.5. At this point, the combined blow was initiated, causing desorption of CO_2 and an increase in the pH solution value. During the test, pH variation is recorded by a pH meter at pre-determined time intervals until equilibrium is reached. It should

Table 1

Good Blowing Pattern

Blowing stage	DBL Ternium BR (m)	DBL LaSiP (m)	Flowrate Ternium BR (Nm^3/minute)	Flowrate LaSiP (Nm^3/minute)	Flowrate TBM Ternium BR (Nm^3/minute)	Flowrate TBM LaSiP (NL/minute)
Decarburization	2.3	0.400	900	120	14	60
End of blow	2.2	0.451	1,200	160	14	60

Figure 3

(a) (b)

Jet penetration (a) and decarburization area (b).

be noted that the experiments were performed in triplicate.

According to Tavares et al. Almeida (2011), a calibration curve is used to convert pH to CO_2 concentration in the solution, using the following relations:

$$A = \frac{pH}{5}$$

$$C_{CO2} = 37294 \times A^{(-14.234)}$$

where A is a conversion constant and C_{CO2} is CO_2 concentration.

The initial concentration (C^{i}_{CO2}), concentration at a certain time t (C^{t}_{CO2}) and equilibrium concentration (C^{eq}_{CO2}) obtained at the end of the experiment (when no longer observed significant variations) were used to draw the calibration curve, through the relation:

$$-\ln\left[\frac{C^{t}_{CO2} - C^{eq}_{CO2}}{C^{i}_{CO2} - C^{eq}_{CO2}}\right] = K_{tm} \times t = G$$

Based on this equation, it is possible to construct a graph of linear behavior and, through the equation of the line, determine the value of K_{tm} (mass transfer coefficient), which represents the axis slope.

Results and Discussion

Mixing Time — Colorimetric Analysis — The interval between the addition time of the tracer occurs to the point where the bath color becomes uniform corresponds to the mixing time.

Tables 2 and 3 present the results of mixing time for each blowing stage, blowing flow, DBL and the tuyere configuration used (TBM), adding the flow of the 12 injection points. It is noteworthy that the experiments were performed in duplicate, in order to validate the results obtained. Thus, the mixing time presented corresponds to the average of the two values found for each experiment and their respective configuration.

Based on the results, it can be observed that the mixing times for the final blow step (160 Nm^3/hour) were lower than the times recorded in the decarburization stage (120 Nm^3/hour). The results obtained may be related to the fact that the lance flow exerts a predominant effect on the progression of the mixture when compared to the DBL and TBM configuration

Table 2

Mixing Times for the Decarburization Stage

Test	Lance flowrate (Nm^3/hour)	DBL (mm)	TBM flowrate (NL/minute) Ext, Int, Central	Mixing times (second)	Standard deviation
TerBR 3-14	120	400	Max, Off, Off (40)	18.25	2.63
TerBR 3-15	120	400	Off, Max, Max (20)	17.00	1.41
TerBR 3-16	120	400	Max, Max, Max (60)	17.75	1.71
TerBR 3-17	120	400	Var, Var, Var (42)	18.50	1.29

Table 3

Mixing Times for the Final Blow Stage

Test	Lance flowrate (Nm^3/hour)	DBL (mm)	TBM flowrate (NL/minute) Ext, Int, Central	Mixing times (second)	Standard deviation
TerBR 3-10	160	451	Off, Max, Max (20)	7.67	1.53
TerBR 3-11	160	451	Max, Max, Max (60)	16.75	1.26
TerBR 3-12	160	451	Max, Off, Off (40)	15.25	1.71
TerBR 3-13	160	451	Var, Var, Var (42)	14.75	1.26

Figure 4

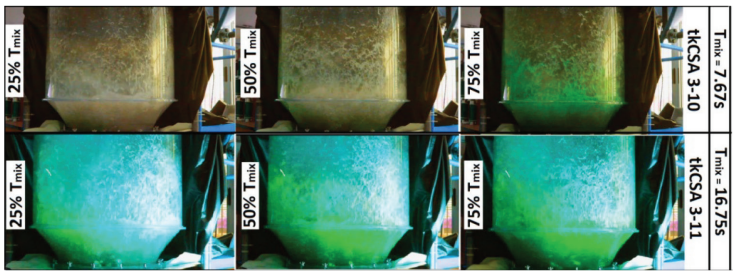

Comparison of tracer behavior.

and flow. Comparing the tests in which the same TBM configurations were used, with different lance flowrates, some similarities can be observed.

The TerBR tests 3-10 and 3-15 (Off, Max, Max–20 NL/minute), for example, showed the lowest mixing times of the final blow and decarburization moments, respectively. From the analysis of the initial behavior of these tests, it is possible to notice that, when injected, the tracer moves to the center of the converter and then undergoes influence of a barrier created by the activated internal tuyeres. However, due to the higher lance flowrate of 3-10 (160 Nm^3/hour), the tracer, upon coming in contact with the combined blow, spreads more vigorously than in the TerBR 3-15 (120 Nm^3/hour), where the tracer tends to follow by the outer crown of the acrylic.

Fig. 4 illustrates the behavior of the tracer during the combined blow for two experiments with similar lance flowrate (160 Nm^3/hour), TerBR 3-10 (20 NL/minute) and 3-11 (60 NL/minute) at three different time points (25%, 50% and 75%).

It is important to mention that for industrial practice the greatest interest is a rapid bath homogenization, even if it is not totally mixed. Thus, the configuration of the TerBR test 3-10 (20 NL/minute) may be more interesting for the post-stirring practice, since for 75% of the mixing time (Tmix) the tracer has been practically taken. In addition, this TBM flowrate is low in relation to the others, causing reduction of inert gas consumption and, therefore, less wear of the refractory, reducing the costs of the process.

Jet Penetration and Decarburization Area — Tables 4 and 5 relate the decarburization area and penetration results for each blow stage, the DBL, and the tuyere configuration used in each experiment.

Taking into account the data recorded in the Tables 4 and 5, it can be noticed that the highest values of penetration were obtained in the tests that used a lance flowrate equal to 120 Nm^3/hour and DBL of 400 mm, when compared to the values measured in the tests with lance flow equal to 160 Nm^3/hour and DBL 451 mm. On the other hand, it was observed that the highest values for decarburization area were

Table 4

Values of Decarburization Area and Jet Penetration to Decarburization Stage

Test	LaSiP DBL (mm)	LaSiP flowrate (Nm^3/hour)	Tuyeres configurations (NL/minute)	Decarburization area (%)	Jet penetration (mm)
TerBR 3-14	400	120	Max, Off, Off (40)	60.42	136.66
TerBR 3-15	400	120	Off, Max, Max (20)	60.45	140.64
TerBR 3-16	400	120	Max, Max, Max (60)	57.89	134.73
TerBR 3-17	400	120	Var, Var, Var (42)	61.34	139.35

Table 5

Values of Decarburization Area and Jet Penetration to Decarburization Stage

Test	LaSiP DBL (mm)	LaSiP flowrate (Nm^3/hour)	Tuyeres configurations (NL/minute)	Decarburization area (%)	Jet penetration (mm)
TerBR 3-10	451	160	Off, Max, Max (20)	66.71	126.46
TerBR 3-11	451	160	Max, Max, Max (60)	69.87	133.17
TerBR 3-12	451	160	Max, Off, Off (40)	64.44	124.51
TerBR 3-13	451	160	Var, Var, Var (42)	66.98	128.58

Figure 5

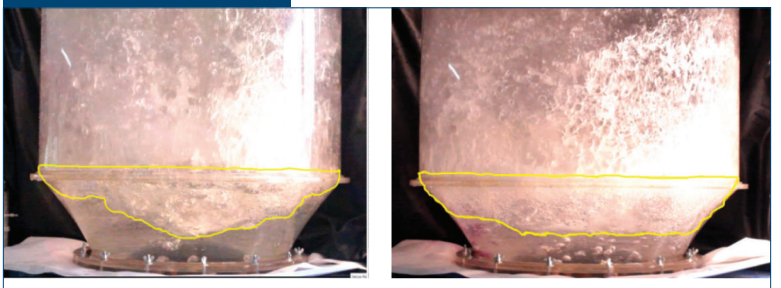

Comparison of decarburization area and jet penetration: TerBR 3-15 – DBL 400 mm and 120 Nm³/hour (a), TerBR 3-13 – DBL 451 mm and 160 Nm³/hour (b).

found in the tests performed with higher lance flow (160 Nm^3/hour) and DBL (451 mm). This behavior can be illustrated in Fig. 5, where two simulated tests with different operating conditions are compared.

By analyzing Fig. 5 and knowing that the demarcated area signals the aspect of the decarburization area and the reach of the jet penetration, some differences are observed.

In letter (a), it can be observed that the jet, because the DBL is smaller, cannot reach a large area of spreading. This leads to smaller decarburization areas and larger jet penetrations. Fig. 6 schematically depicts the location of jet impact in both cases.

In the case of letter (b), a test is characterized in which the presence of dead zones in the sides of the acrylic is minimized by the amplitude of the reach of the jet. Since the DBL and the flowrate are larger in this case, the jet interacts, on impact, with a larger bath area that offers superior resistance to penetration, increasing the amount of bubbles and the water-gas contact surface area (MAIA, 2007). Thus, the configuration of tests with a top flowrate 160 Nm^3/hour may be more suitable for dephosphorization in primary refining and may potentially represent an attack on the trunnion line.

By means of an analysis focused on the influence of the tuyeres on the jet penetration and the decarburization area, it is possible to observe in the tests related to the final blow step (160 Nm^3/hour) an interesting behavior in which the external radii were connected. Due to the greater jet range in the lateral parts of the acrylic caused by the higher DBL in these tests, a hypothesis is generated of a possible impact between the jet and the bubble pen coming from the external radius tuyeres, causing a reduction in the size of the decarburization area and jet penetration. This hypothesis is illustrated by the fact that the lower values of jet penetration and decarburization area are related to the TerBR test 3-12, in which only the external radius tuyeres were in operation. In addition, it is worth mentioning that the results found for the TerBR 3-10 test (internal and central radius driven) were higher than those of TerBR 3-12, leading to a probable preponderance of internal and central radius tuyeres in relation to the external radius ones and, therefore, optimizing the process economy, since the consumption of injected gas is significantly lower.

In the case of tests related to decarburizing step (DBL 400 mm), it was observed that the values of decarburization area were very similar. This similarity of results leads to a probable analysis that the tuyeres did not represent significant influence in the experiments in front of the flowrate of the jet. Thus, with regard to process economics, the configuration used in the TerBR 3-15 test, where the flowrate of the tuyeres is minimal and the results for area of decarburization and jet penetration are satisfactory, is highlighted.

Figure 6

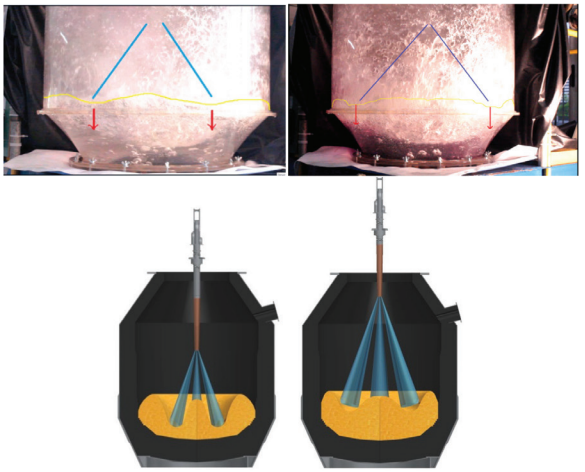

Jet impact location.

CO_2 Desorption — The aim of desorption is to represent the rate of decarburization in refining processes, especially in the final stages, when the reactions occur through diffusion of the gas in the medium. Fig. 7 shows the behavior obtained for two experiments.

From Fig. 7, it is possible to note that the decay rate of the CO_2 concentration was more pronounced for the TerBR 3-8 experiment. This fact can be justified because its total blowing flow (162.52 Nm^3/hour) is higher than that of the TerBR 3-4 experiment (121.2 Nm^3/hour). The upper flow is responsible for causing a greater mass movement, which favors the kinetics of the reactions. Thus, an increase in the flowrate is

recommended in industrial practice, in order to intensify the decarburization.

Considering the values of pH and [CO_2] during the blow, a first-order kinetic equation was generated, so that the slope of the line represents the mass transfer constant K_{tm}, as shown in Fig. 8.

Considering the slope presented by the graph in each experiment, it was possible to obtain the values of "K_{tm}" for each configuration analyzed. It is noteworthy that the experiments were performed in triplicate.

The mean K_{tm} values and the respective standard deviations are shown in Table 5.

From the values recorded in Table 5, it is possible to notice that the experiments with lance flowrate of 160 Nm^3/hour showed higher values of K_{tm} when compared to those registered by the tests that used a flowrate of 120 Nm^3/hour. In this way, the tests with greater lance discharge showed an increase in the bath movement mass, favoring the last stage of decarburization. In view of these results, it is evident the greater influence of the blow by the top on the mass transfer, as can be seen when comparing the K_{tm} values obtained in the tests TerBR 3-3 and TerBR 3-5, which, despite having a lower TBM flow, presented a higher value for the constant K_{tm}.

In addition, it is worth mentioning the behavior presented by the TerBR 3-8 and TerBR 3-4 experiments, both with configuration of the tuyeres with a flowrate of 20 NL/minute. When analyzing the values of the mass transfer constant of these experiments, it is observed that these values are quite equivalent to the values of other experiments that used higher flowrates. For example, the TerBR 3-8 experiment had a mass transfer constant greater than that of the TerBR 3-2 experiment, both simulating the blow end. However, the TBM outflow from experiment 3-2 is twice as high as the flow from experiment 3-8. This is an economically important point, since the lower the flow used, the lower the operating costs. In the case of simulation of decarburization, experiment 3-4 (flow TBM 20 NL/minute) presented higher value of the mass transfer constant than experiment 3-5 (flow TBM 60 NL/minute). Therefore, with a lower flowrate and, consequently, lower costs, satisfactory results were obtained.

Figure 7

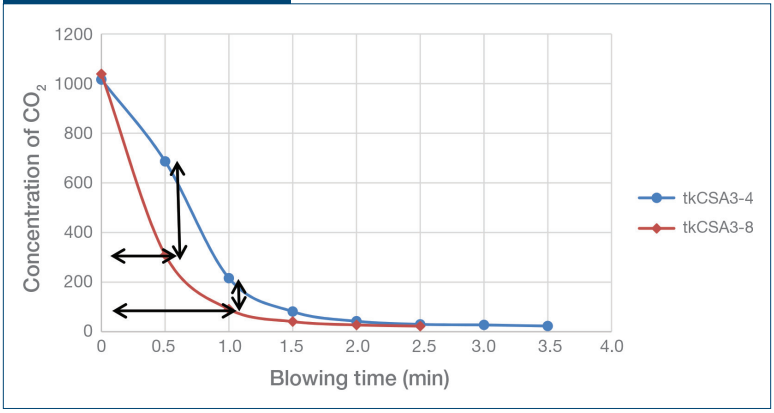

CO_2 concentration x blowing time (blue TerBR3-4; red TerBR3-8).

Figure 8

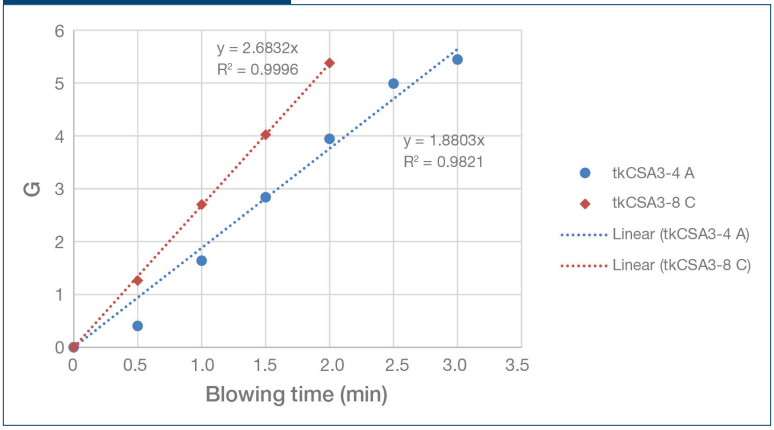

G x Blowing time (blue TerBR 3-4A; red TerBR 3-8A)

Table 5

Mean K_{tm} Values for Each Experiment

Test	Lance flowrate (Nm^3/hour)	TBM flowrate (NL/minute)	Total flowrate (Nm^3/hour)	Mean K_{tm}	Standard deviation
TerBR 3-9	160	42	162.52	2.460	0.149
TerBR 3-8	160	20	161.2	2.425	0.222
TerBR 3-7	160	60	163.6	2.568	0.166
TerBR 3-2	160	40	162.4	2.349	0.160
TerBR 3-3	120	40	122.4	1.977	0.242
TerBR 3-4	120	20	121.2	1.902	0.025
TerBR 3-5	120	60	123.6	1.849	0.234
TerBR 3-6	120	42	122.52	1.934	0.157

By means of an analysis focused on the influence of the tuyeres (TBM) in the CO_2 desorption process, no relation was observed between the total flowrate and the value of the mass transfer constant. In contrast, it can be seen that the configuration of the tuyeres

has a significant importance in the value of K_{tm}. In the case of the tests of the end of the blowing stage, it was observed that the internal radius and the central tuyeres present greater influence on the K_{tm} value. This fact can be highlighted by comparing the TerBR 3-9, TerBR 3-8 and TerBR 3-7 tests in relation to the TerBR 3-2 experiment, in which only the external tuyeres were activated. It was observed that the highest values of K_{tm} were reached by the tests in which the internal and central radius tuyeres were used. It is worth noting the TerBR 3-8 test (external radius off), in which the mass transfer constant obtained was higher than the K_{tm} of the TerBR 3-2 experiment (internal and central radius off).

Figure 9

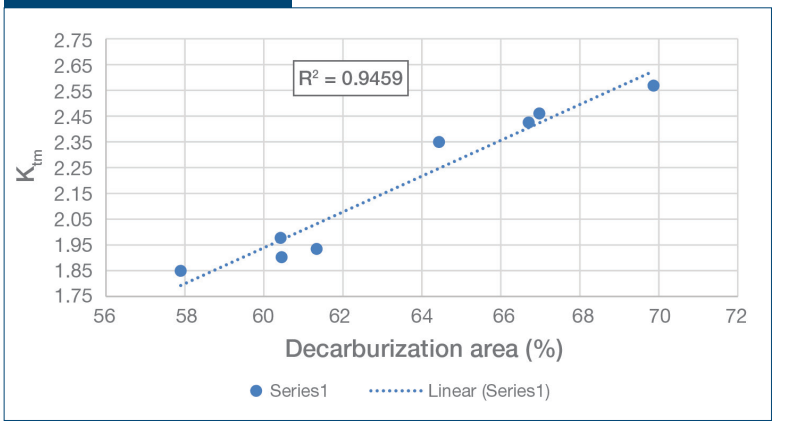

K_{tm}x decarburization area.

On the other hand, the experiments of the decarburization stage presented different behaviors. One possible explanation concerns the different bath lance distances. With the decrease of DBL, the jet reaches a smaller surface area of the bath (impacting predominantly the central region), which can interfere negatively in the action of the internal and central radius tuyeres. This can be demonstrated by the fact that the largest mass transfer constant was obtained for the TerBR 3-3 test, in which only the outer radius tuyeres were connected.

Another approach refers to the comparison between the mass transfer constant and the decarburization area, which can be illustrated by Fig. 9.

By analyzing the graph in Fig. 9, it is possible to verify that the larger the decarburization area, the higher the mass transfer constant. This relationship can be explained by the increase in the probability of occurrence of chemical reactions when raising the decarburization area.

Conclusions

From the various means of analysis used during the experiments, the following conclusions were obtained:

1. The lance flowrate is predominant in determining the bath homogenization compared to the other parameters. In relation to the TBM, the experiments with configuration of external radius off and the internal radius connected to the maximum flowrate showed the lowest mixing times for the two simulated stages (decarburization and final blow).
2. For a higher lance flowrate, the jet reaches a longer range along the acrylic, which allows a clash between the jet and the bubble lance from the external radius, causing a reduction in the size of the decarburization area and penetration. The highest values for the basin were obtained in the experiments with higher lance and DBL.
3. Superior lance flowrates are responsible for a greater mass movement, which favors the kinetics of the reactions. In relation to the TBM, the configuration of internal radius tuyeres and the central one operated at maximum flow had a greater influence on the value of K_{tm} in relation to those of connected external radius. However, for lower values of DBL, the K_{tm} is higher when the external ones are activated, since the jet interferes negatively in the action of the central and internal tuyeres.
4. It was verified that the largest values of the mass transfer constant correspond to the experiments with the largest decarburization area, which validates the theory that larger impacted areas allow the greater occurrence of chemical reactions.
5. The results obtained for DBL 0.400 m show that the tuyeres, regardless of the configuration, have a lower influence on the decarburization area and the penetration when compared to the results for DBL 0.451 m. This represents an opportunity to optimize operations by using the minimum settings in TBM.
6. All of the analyses concluded above lead to a possible hypothesis that the best configuration of tuyeres would be the one with external tuyeres off and the central and internal ones operated at the maximum flowrate (20 NL/minute). This configuration has benefits for the industrial process, since it allows for good metallurgical results to be achieved using minimum flow of TBM, reducing the operational costs from the saving in consumption of inert gas and, consequently, the wear of the refractory.

Acknowledgments

The authors thank the Universidade Federal de Minas Gerais for providing the dependencies of Process Simulation Laboratory – LaSiP and the inputs for the tests. They also thank Ternium Brasil and Lumar Metals for encouraging continued research and support.

References

1. Almeida, L.P., et al., "Effects of Some Operational Parameters Upon Degasification Rate, Mixing Time, Splashing and Skull Development in a Combined-Blow Converter During Steelmaking Refining: A Physical Model Approach," *AISTech 2010 Conference Proceedings,* Vol. I, 2010, pp. 274–285.
2. Maia, B.T., "Physical and Mathematical Modeling of Fluid Flow Within Basic Oxygen Converters and in the EOF Process Evaluation of Different Configurations of Oxygen Injection Lances (in Portugese)," dissertation, doctorate in metallurgical engineering, Universidade Federal de Minas Gerais, 2013.
3. Maia, B.T.; Faustino, R.A.; Abreu, G.; Costa, B.; and Tavares, R.P., "Effects of the Support Parameters in the Time of Misture Using the Physical Model of the Converter (in Portugese)," *44th International Steelworks Seminar,* Araxá, Minas Gerais, 2013.
4. Maia, B.T.; Petrucelli, A.C.; Diniz, C.N.A.; Silveira, D.; Andrade, P.H.M.S.; Imagawa, R.K.; and Tavares, R.P., "Comparison of Oxygen Blow Penetration in BOF Converters With Multi-Purpose Nozzles Using Physical Modeling (in Portugese)," *International Steelworks Seminar,* Porto Alegre, RGS, Brazil, 2014.
5. Seshadri, V.; Tavares, R.P.; Silva, C.A.; and Silva, I.A., *Transport Phenomena: Foundations and Applications in Metallurgical and Materials Engineering,* Associação Brasileira de Metalurgia, Materiais e Mineração, São Paulo, Brazil, 2010, p. 812.
6. Szekely, J., and Themelis, N.J., *Rate Phenomena in Process Metallurgy,* 1st ed., John Wiley & Sons, Montreal, Que., Canada, 1971, p. 784.
7. Tavares, R.P., "Mass Transfer in Steelmaking Operations," Universidade Federal de Minas Gerais, 2011. ✦

This paper was presented at AISTech 2017 — The Iron & Steel Technology Conference and Exposition, Nashville, Tenn., USA, and published in the Conference Proceedings.